Fabrication and characterization of carbon-based nanostructured electrodes for Microbial Fuel Cells (MFCs).

Miguel Fernández-Martín
Roger Amade[1,2], Enric Bertran-Serra[1,2]

[1] ENPHOCAMAT (FEMAN) Group, Dep. Applied Physics, Universitat de Barcelona, C/ Martí i Franquès, 1, 08028, Barcelona, España

[2] Institute of Nanoscience and Nanotechnology (IN2UB), Universitat de Barcelona, Diagonal 645, 08028, Barcelona, España

***Abstract*—. Microbial Fuel Cells (MFCs) are bioelectrochemical systems that can produce bioelectricity from organic matter. Wastewater from urban, domestic or industrial origin can be used as a fuel to produce electricity. In addition, the amount of pollutants and contaminants decreases during the production of bioelectricity. Thus, such bioelectrochemical systems produce renewable energy and, simultaneously, can be used as a novel technology for wastewater treatment. However, the efficiencies obtained are still too low and the output voltage of the MFCs need to be increased. Furthermore, the overall cost of the cell must be reduced in order to promote this technology into the market. Here, we have studied the growth of graphene nanowalls (GNWs) on stainless-steel substrate 304 (SS), which can be used as electrodes in air-cathode MFCs. Growth parameters have been optimized to obtain dense carbon nanostructures on both SS foil and mesh. MFCs with different electrodes have been prepared to study the effect of different parameters and to determine whether the presence of carbon nanostructures results in an increase of the electrochemical efficiency. An oxygen plasma treatment has been performed to study its effect on the properties of the electrodes. Finally, MnO_2 has been electrochemically deposited to determine its catalytic effect in the oxygen reduction reaction (ORR) that takes place on the cathode. Results show an increase in the output voltage and power density when GNWs electrodes are compared to MnO_2 bare electrodes, with a maximum power density of 9 mW/m^2. Moreover, the influence of the oxygen plasma post-treatment, performed on the nanostructures, over microbial communities developed as biofilm in the anode is demonstrated. Overall, this study shows the potential of GNWs to increase the yield of MFCs.**

***Index Terms*—7. Nanoenergy: microbial fuel cells, carbon-based electrodes, PECVD, electrochemical properties.**

I. Introduction

BY definition, a fuel cell (FC) is an electrochemical apparatus that turns the chemical energy of a fuel into electrical energy without fuel combustion . Hence, FC is an electrochemical energy conversion device [1]. The name comes from the production of electricity from a fuel external supply (on the anode side) and an oxidant one (on the cathode side). This reaction takes place in presence of an electrolyte.

Theoretically, FC can produce electricity continuously as long as the necessary flows of fuel and oxidant are maintained. This is an important difference from batteries, who store electrical energy in a closed system, but it is not the only one. While the electrodes within a battery react and change as a battery is charged or discharged, fuel cell's electrodes are catalytic and relatively stable [2].

Nowadays, FCs have many applications, mostly focused on portable power generation, stationary power generation [3], and power for transportation [4]. Depending on the application and also on different parameters such as: type of reactants, operating conditions (temperature and pressure), or the electrolyte used, FCs can be classified in many different ways. In this case, we put the spotlight on biological FCs, that convert the chemical energy of carbohydrates into electric energy [5].

At the anode, a fuel (e.g., glucose) is oxidized according to the reaction:

$$C_6H_{12}O_6 + 6H_2O \rightarrow 6CO_2 + 24H^+ + 24e^-,\ E^\circ = 0.014\ V \quad (1)$$

At the cathode, oxidant is reduced by the presence of a catalyst (e.g., oxygen):

$$6O_2 + 24H^+ + 24e^- \rightarrow 12H_2O,\ E^\circ = 1.23\ V \quad (2)$$

The main distinguishing feature, central to a biological FC, is the use of the living organism itself as energy productor, in our case microbes accumulated in the anode as a biofilm. This type of devices where current is generated due to the action of microorganisms, by transferring electrons from a reduced electron donor to an electron acceptor at a higher electrochemical potential are called microbial fuel cells (MFCs) [5].

The performance of MFCs is mainly attributed to the anode

behavior since cathodic reduction could be considered as stable (abiotic), and not exposed to the shifts in microbial metabolism [6]. Therefore, the suitability of a MFCs device is normally determined by the composition, morphology, and surface properties of anode materials. These facts exert a strong influence in fundamental parameters in the overall process such as: bacteria attachment, electron transfer, and substrate oxidation of the electrode. However, MFCs depends on both anode and cathode overpotentials (activation losses, bacterial metabolism losses, and concentration or mass transport losses). Hence, the more efficient the electrodes, the more effective will be the MFC in terms of power production [7].

Recently, it has been proved that the modification of the electrode surfaces with nanomaterials, specially based on carbon materials such as carbon nanotubes (CNTs) [8], graphene [9], graphene oxide (GO) [10] and reduced graphene oxide (rGO) [11] shows greater electrochemical performance as well as higher power density in MFCs than former materials, providing a better electronic transfer and a larger surface-to volume ratio. Regarding this wide range of carbon nanostructures, graphene is considered as the most promising material due to its electronic, mechanical, and conducting properties [12]. Moreover, graphene has a high specific surface (theoretical value of 2600 m^2/g) and it is well-known by its low production cost, and easy functionalization and processing [13].

Among the different types of possible graphene nanostructures, graphene nanowalls (GNWs) is one of the most recently developed and less investigated material. GNWs, Fig. 1, can be described as self-assembled, vertically standing, few-layered graphene sheet or wall nanostructures, which are also called as carbon nanowalls or carbon nanosheets [14].

The graphene walls constituting the material are normally produced with thicknesses in the range from a few nanometers to a few tens of nanometers, depending on the method and conditions. The large surface area of GNWs provides an interesting application in the electrochemical field to this material, from electrodes for energy storage devices to biosensors [15]-[17]. Concerning FCs, GNWs have been explored as a potential catalyst support material especially in proton exchange membrane fuel cells (PEMFCs) for Pt catalysts. However, metal nanoparticles are deposited only around the tops of GNWs and tend to easily clump together, resulting in the formation of larger particles or films on top of the nanostructures [18].

During this experiment, GNWs were grown by plasma-enhanced chemical vapor deposition (PECVD) on different stainless-steel (SS) substrates, mesh and foil, in order to improve the performance of both electrodes, anode and cathode, by increasing the specific surface area. In addition, MnO_2 was electrochemically deposited coating the surface of some cathodes to evaluate its performance acting as a catalyst for the oxygen reduction reaction (ORR). Finally, the effect of an oxygen plasma treatment on the properties of the electrodes was investigated.

To the best of our knowledge, the use GNWs and GNWs/MnO_2 nanocomposites deposited on different stainless-steel electrodes, mesh and foil, in MFCs has not been reported before. The use of both electrodes based on stainless steel results on a significantly reduction in terms of cost in the device production. A single compartment MFC was constructed and tested using wastewater from a local wastewater treatment plant (WWTP) called Estació depuradora d'aigües residuals (EDAR) Sant Feliu de Llobregat [19].

II. ELECTRODES PREPARATION

A. Carbon nanostructures growth by PECVD

As mentioned previously, costs reduction of devices is a real need in the electrochemical field, and MFCs are not an exception. The use of cost-effective current collector materials such as SS as electrodes are considered as a good option since the overall cost of the bioelectrochemical systems is decreased. SS substrates have the advantages of being flexible, relatively chemically stable, and with low resistance [20].

In this case, GNWs have been grown on SS 304 by the inductively coupled plasma enhanced chemical vapor deposition (ICP-CVD) method. Among the several methods for synthesizing GNWs, ICP-CVD is one of the most promising techniques since the synthetic route can be performed at relatively low temperatures.

The ICP-CVD is a very common path to synthesize carbon nanostructures, included in the PECVD techniques. This type of techniques arises from the combination of Chemical Vapor Deposition (CVD) and Physical Vapor Deposition (PVD).

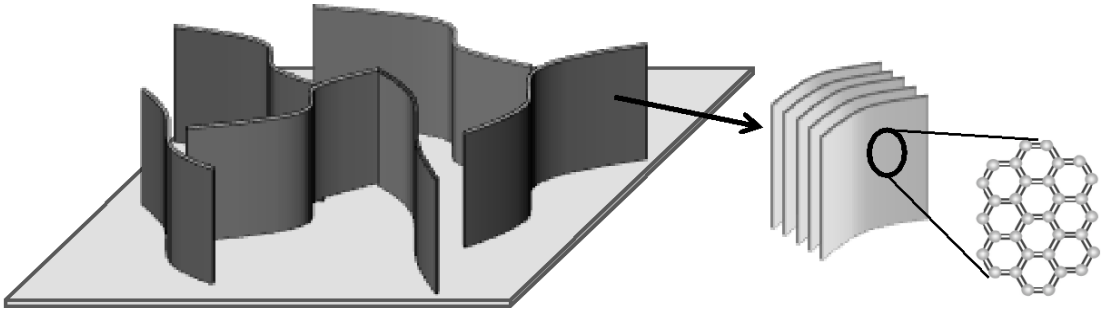

***Fig. 1**. Schematic illustration of graphene nanowalls (GNWS) [13].*

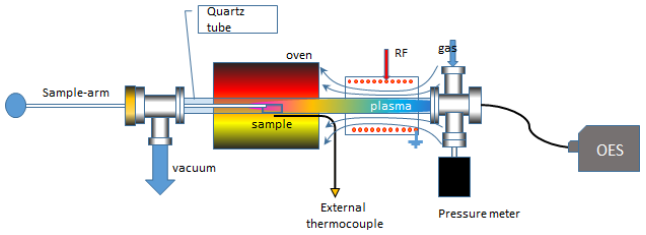

Fig. 2. *Schematic drawing of the ICP-CVD tubular reactor for producing carbon nanostructures. The reactor is composed of a quartz tube, an oven, and a coil connected to an RF power supply. The sample is placed in the middle of the oven. The system is evacuated with a primary rotatory pump and the pressure is monitored by a capacitive pressure meter. The temperature is measured by means of two thermocouples. Different gases can be introduced through an inlet at one end of the quartz tube. An Optical Emission Spectroscopy (OES) study could be performed during the deposition process to investigate the generated species.*

The plasma action provides a rich chemical environment, including radical mixtures, molecules and ions form a simple hydrogen-hydrocarbon feedstock. Hence, the efficient dissociation of gas molecules at low temperatures by the action of the plasma energy is the main reason to perform the synthetic paths at relatively low temperatures [21].

The GNWs growth process can be divided into two main nucleation stages. Initially, the first nucleation results in a buffer layer formation, containing a high number of defects such as amorphous carbon. The growth rate of GNWs depends on this buffer layer and is considered as one of the main requirements to obtain good quality GNW-structures. Once the buffer layer formation is finished, the secondary nucleation stage occurs resulting in the vertical alignment of the graphene nano-sheets [21].

In this case, GNWs were synthesized on the SS substrates, both foil and mesh, using the ICP-CVD system that can be seen in Fig. 2. The ICP-CVD system (13.56 MHz, power 440 W) consists on a long quartz tube, a radiofrequency (RF) resonator for producing remote plasma, and a tubular oven, that could work up to 1100 °C, placed 20 cm away from the quartz tube.

In the GNWs synthesis is important to distinguish between SS-mesh samples (about 200 µm thick) and SS-foil samples (100 µm thick) since they are not equal in terms of morphology and this fact could induce difference in the first nucleation stage of the growing process.

TABLE I
GNWS SYNTHESIS OVER DIFFERENT SUBSTRATES

Experimental conditions		MFC cathode (SS-mesh)	MFC anode (SS-foil)
H_2 reduction treatment	H_2 flow	13 sccm	13 sccm
	Ar flow	13 sccm	13 sccm
	Power	90 W	200 W
	Pressure	100 Pa	100 Pa
	Temperature	730°C	730°C
	Time	600 s	300 s
GNWs growth	CH_4 flow	13 sccm	13 sccm
	Power	400 W	400 W
	Pressure	40 Pa	40 Pa
	Temperature	750°C	750°C
	Time	1800 s	1800 s

sccm = standard cubic centimeter per minute, °C=Celsius.

In order to compensate these differences in the structure, caused mainly by the material production and the thickness of the sample, some experimental parameters such as time or plasma power were tuned depending on the type of sample used, see Table I.

Unlike CNTs growth, GNWs can be synthesized on a stainless-steel substrate without the use of catalysts [22]. However, a pre-treatment based on reducing atmospheres, containing gases such as NH_3 or H_2, is commonly used since it facilitates the production of graphene nanostructures. The pre-treatment reduces the native oxide layer present on the substrates, mainly Cr_2O_3 when we are dealing with SS samples, allowing the formation of the amorphous carbon layer that will induce the GNWs obtention during the first nucleation stage. In this case, the reducing atmosphere were based on a gas mixture of H_2 and Ar, as seen in Fig 3.

The experimental synthetic process began with the sample introduction inside the quartz tubular reactor, which was evacuated down to a pressure below 1 Pa and heated up to 730°C. Then, H_2/Ar atmosphere was generated introducing 13 sccm of each reactant and the pressure was maintained in the range of 100 Pa. Under these conditions, plasma was ignited at a RF power of 90 W during 10 min for SS-mesh acting as substrate and 200 W during 5 min for SS-foil substrates.

As it can be seen in Fig. 3, the morphology of the SS substrate changes during the reductive treatment. The crystals growth induces the deterioration of the mechanical properties.

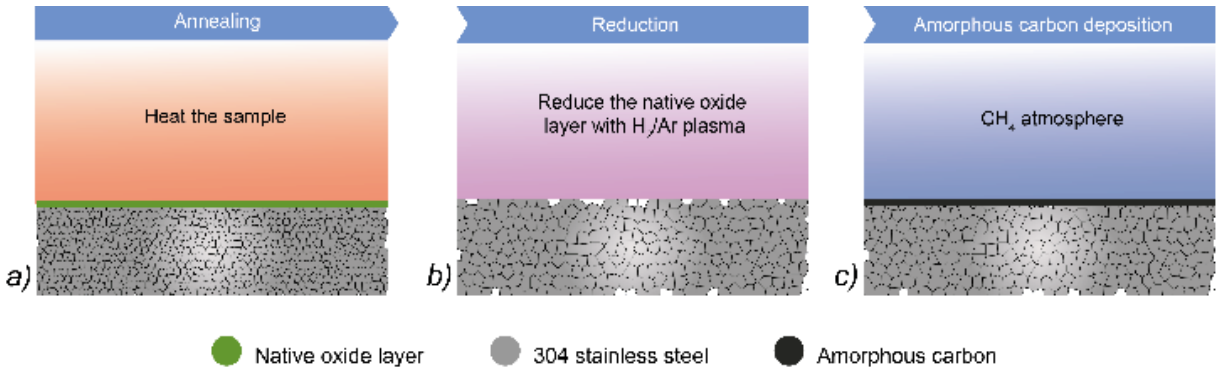

Fig. 3.*. Pre-treatment based on reducing atmospheres used before the GNWS synthesis to eliminate the native oxide layer of the substrate.*

Furthermore, carbide precipitation occurs at the surface and at the grain boundaries, decreasing the corrosion resistance of the material. This phenomenon is known as *sensitization* and could induce the loss of the electrochemical properties in our sample. For this reason, it is extremely important the adjustment of the experimental conditions to each substrate in order to remove the native oxide layer present on the SS surface minimizing the damage in the material.

Once the pre-treatment was finished, the GNWs synthesis started. Then, pure methane (99.995%) was introduced as a precursor gas at one end of the quartz tube (13 sccm) and the pressure was maintained in the range of 40 Pa. Under these conditions, plasma was ignited at a RF power of 400 W for 30 min. Lastly, the sample was cooled down to room temperature for 30 min.

In addition to the synthesis of GNWs, the determination of the action of the plasma post-treatments over these structures was one of the aims of this work. These treatments are frequently used to clean and modify the surface of materials, including polymers and carbon-based materials, since they result in an enhancement of the electrochemical properties.

Oxygen plasma treatment removes surface impurities and increases the surface oxygen functionalities. The increase of the oxygen functionalities induces an improvement of the wettability properties of the GNWs. Wettability could be influenced by the chemical composition, the geometric structure, or both [23]. Usually, GNWs show poor wettability due to the effect of the vertical orientation of graphene in their geometric structure [21]. Therefore, this oxygen plasma post-treatment should decrease the hydrophobicity of the GNWs electrodes, see Fig. 4, resulting in a reduction of the reaction rate losses regarding reactants consumption at the electrode by the electrochemical reaction. Furthermore, this post-treatment generates step-like defects, that are well-known for providing numerous edge planes, which exhibit fast electrochemical kinetics [24].

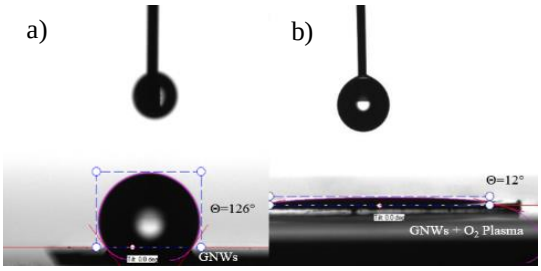

Fig 4. *Contact angle shift on GNWs surface from 126º (a) to 12º (b), after applying 20 s of O_2 plasma [21].*

TABLE II
GNWS SYNTHESIS OVER DIFFERENT SUBSTRATES

Experimental conditions		MFC electrode SS-mesh / SS-foil
O_2 plasma treatment	O_2 flow	13 sccm
	Power	50 W
	Pressure	40 Pa
	Temperature	20-25ºC
	Time	30 s

sccm = standard cubic centimeter per minute, ºC = Celsius.

In other words, a more effective MFC system in terms of power production could be build up due to the plasma post-treatments performed after the carbon nanostructures growing processes.

In this case, oxygen plasma treatment was performed in the same reactor system used for GNWs growth. The reactor was first evacuated to a base pressure of less than 10^{-3} Pa before the plasma gas was introduced. Then, the sample was placed in the center of the reactor and exposed to O_2 plasma in the RF plasma reactor at a constant system pressure of 40 Pa at a flow rate of 10 sccm. The oxygen plasma treatment was performed at 50 W of plasma power for a period of 30 sec. All the procedure was performed at room temperature. In Table II, these experimental conditions for the performed oxygen plasma over MFCs GNWs-based electrodes are summarized.

B. MnO_2 electrodeposition

In order to determine the effect of MnO_2 catalyst in the O_2 reduction reaction resistance at the cathode side, MnO_2 was electrochemically deposited on the SS-mesh with and without carbon nanostructures. Different methods such as hydrothermal [25], sol gel methods [26], [27], and electrodeposition [28] can be used to deposit and prepare MnO_2.

In this case, and due to the excellent results in similar samples, vertically aligned carbon nanotubes (VACNTs), previously obtained by the *FEMAN* research group [7], the selected procedure consists of an anodic deposition based on electrolyte solutions.

Anodic electrodeposition consists on the oriented diffusion of charged reactive species through an electrolyte when an electric field is applied. Then, oxidation of the charged species occurs on the electrode, also known as deposition surface [20]. For the anodic electrodeposition of MnO_2, typically used in a wide range of electrochemical devices, the oxidation of Mn(II) species occurs on the anode surfaces, following the next equation:

$$Mn^{2+} + 2H_2O \rightarrow MnO_2 + 4H^+ + 2e^- \; E^\circ = -1.23\ V \qquad (3)$$

The electrodeposition of MnO_2 was performed using a galvanostatic method over the SS-mesh electrodes, which will act as cathode in the MFCs system. The method consists on using these SS-mesh electrodes, with or without GNWs, as the anode and a graphite electrode as the cathode in a 0.1 M Na_2SO_4 aqueous solution with about 6 cm separation between electrodes. The device used to carry out the experiment was the same as for the MFCs setup. About 0.5 cm^3 of a 0.2 M $MnSO_4 \cdot H_2O$ solution was added drop wise to the electrolyte through a hole in the cathode applying 1 $mA \cdot cm^{-2}$ for 2 min, which resulted in the electrodeposition of a thin layer of MnO_2 onto the sample surface.[29]. The experimental conditions for the electrodeposition process are summarized in Table III.

TABLE III
MnO_2 electrodeposition

GALVANOSTATIC METHOD	
Cathode	Graphite
Anode	SS-mesh / SS-mesh + GNWs
Electrolyte solution	35.0 mL $NaSO_4$ (0.1 M)
Deposit Solution	0.5 mL $MnSO_4$ (0.2 M)
Set current	5.3 mA
Anode area	5.3 cm^2
Current density	1 mA · cm^{-2}
Time	120 s

mL = milliliter, M = molarity.

III. ELECTRODES CHARACTERIZATION

A. *Electron microscopy- FE-SEM*

As it has been described before, GNWs consists of graphite sheet nanostructures with edges that are composed of stacks of graphene sheets standing almost vertically onto the substrate.

The self-supported network formed by carbon sheets could be characterized using electron microscopy, both scanning electron microscopy (SEM) and transmission electron microscopy (TEM), since the generated structures have thicknesses in the range from a few nanometers to a few tens of nanometers, and with a high aspect ratio.

In our case, the structure and morphologies of the grown GNWs samples synthesized using ICP-CVD were firstly characterized using a field emission scanning electron microscopy (FE-SEM) (JEOL JSM-7001F, operated at 20 kV, JEOL Ltd., Tokyo, Japan)

Figure 5 shows different top view images of bare GNWs grown on SS-mesh substrate. As shown in the top images with low magnification values, the nanowalls are homogeneously distributed along the sample. In the next two images their open structure with voids between the nanowalls can be seen, and the length, several hundreds of nanometers, and the thickness, a few nanometers, can be determined.

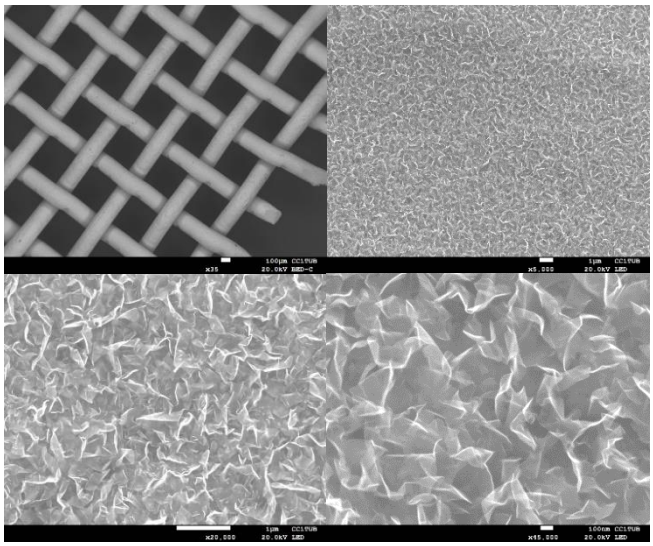

Fig 5. *Characterization performed via Field-Emission Scanning Electron Microscopy in the measurement facilities of Centres Científics i Tecnològics de la Universitat de Barcelona (CCiTUB). Mesh with 200µm diameter SS wire, 383×383 µm² aperture (38.6% aperture).*

This procedure was repeated in all the samples in order to ensure the reproducibility of the synthetic process on both substrates.

The morphology and the structure of the GNWs depend on the source gases, pressure, process temperature, as well as the type of plasma used for the synthesis. It is important to mention that in the case of the SS-foil as substrate, we took advantage from the previous work of the *FEMAN* research group using the same substrate and reactor system [20]. Nevertheless, the SS-mesh had not been used as substrate previously in the reactor system and thus, the experimental conditions on both processes, H_2 reduction pre-treatment and GNWs growth, were adjusted to obtain such a homogeneity.

B. *Raman Spectroscopy (2013)*

The obtained Raman spectrum for GNWs grown on SS substrate is shown in Fig. 6 a). Typical Raman spectrum for the GNWs has G band peak at 1590 cm^{-1} indicating the formation of a graphitized structure and D band peak at 1350 cm^{-1} corresponding to the disorder-induced phonon mode.
The peak intensity of D band is twice as high as that of G band. The G band peak is accompanied by a shoulder peak at 1620 cm^{-1} (D' band), which is associated with finite-size graphite crystals and graphene edges [30], [31].

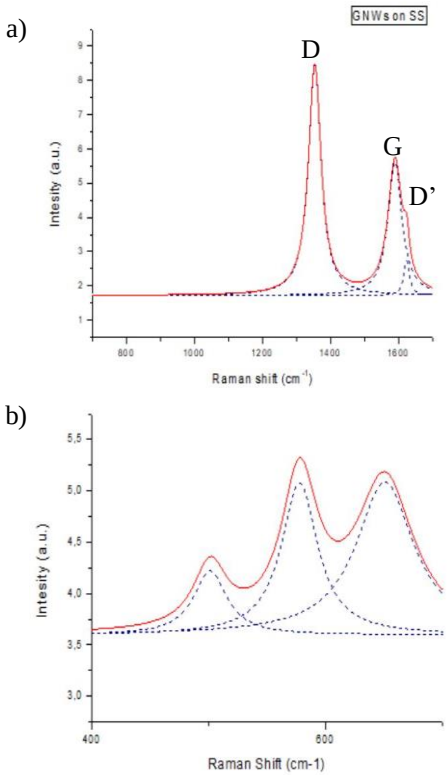

Fig 6. *A) GNWs on SS. B) MnO_2 on SS. Characterization performed via Raman technique (HORIBA, labRam HR800, Japan) using a green laser of 532nm wavelength, 0.8 mW power, and a ×10 objective in the measurement facilities of Centres Científics I Tecnològics de la Universitat de Barcelona (CCiTUB).*

The strong and sharp D band peak and D' band peak suggest a more nanocrystalline structure and the presence of graphene edges and defects, which are prevalent features of GNWs [13].

In fact, the I_D/I_G ratio is used to evaluate the defect formation along the GNWs surface reveling the defects formed during the primary and secondary nucleation and growth of the carbon nanostructures. The $I_D/I_{D'}$ ratio is also important since it provide us the on-site and boundary-like defects information [8].

In Fig. 6 b), three Raman bands located at 501, 570, and 640 cm^{-1} for the MnO_2 electrodeposited onto SS-mesh can be seen. These results are in good agreement with the three major vibrational features of the MnO_2 compounds previously reported at 500 to 510, 575 to 585, and 625 to 650 cm^{-1} [32].

IV. Experimental Setup

During the experiment, the system used to perform the electrochemical measurements consisted of an air-cathode single compartment MFC with a cylindrical plastic chamber (5.0 cm long, 5.4 cm diameter) and an empty volume of 35 mL. The MFCs contain two plastic caps that were used to close the cell. One of the caps has an aperture (2.6 cm diameter) for the air-breathing cathode [7].

The air-porous cathode consisted of a SS-mesh with three possible configurations, see Table IV, and a proton exchange membrane (PEM) mechanically pressed to the SS-mesh by five bolts attached to the plastic caps of the MFC. The effective geometrical area of the air-breathing cathode was 5.3 cm^2, see Fig 7.

The anode consisted of GNWs grown on a SS-foil substrate with two possible configurations regarding the plasma treatment, see Table IV, and with the same effective geometrical area than the air-cathode. However, the anode requires a higher surface area than the cathode in order to promote the formation of a microbial biofilm that can transfer electrons to the anode during digestion of waste matter. For that reason, the nanostructured substrates based on GNWs are found to increase the performance of MFCs due to the high specific area of this carbon structures.

Two VITON® rings, one at each electrode, were used to seal the chamber, which was filled with wastewater from the primary clarifier effluent of a municipal WWTP (EDAR Sant Feliu de Llobregat, Spain) [19]. The water was stored at 4 °C and used within 3 weeks after collection.

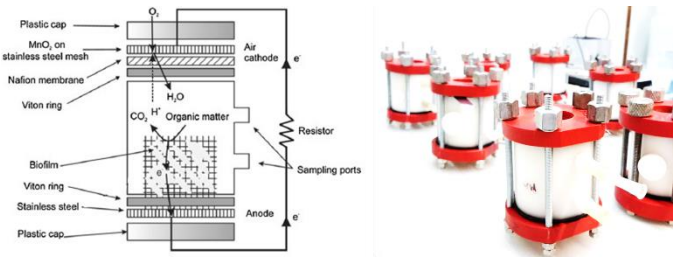

***Fig 7.**. Scheme and photograph of the air-cathode single chamber MFCs. The oxidation of the organic matter catalyzed by the microorganisms takes place at the anode generating protons, electrons, and CO2. At the cathode side, oxygen from the air is reduced by the electrons and protons forming water molecules*

TABLE IV
MFC EXPERIMENTAL SETUP DESIGN

MFCs	Cathode (SS-mesh)	Anode (SS-foil)
A.1 A.2	MnO_2	GNWs + O_2 Plasma
B.1 B.2	MnO_2 / GNWs + O_2 Plasma	GNWs + O_2 Plasma
C.1 C.2	GNWs + O_2 Plasma	GNWs + O_2 Plasma
D.1 D.2	GNWs + O_2 Plasma	GNWs

The four electrode configurations were prepared per duplicate, in order to average the values in the final report, since the behavior of microorganisms in MFCs can involve several complex processes and the reproducibility is affected.

In Table IV, the four different electrode configurations prepared in order to analyze the effect of the GNWs on the electrodes and their functionalization are summarized.

V. Electrochemical Measurements

In order to perform the electrochemical measurements, the cells were fed with wastewater from the primary clarifier effluent for 40 days to develop a microbial biofilm in the anode and deliver a stable voltage.

During this period, the two MFC electrodes were connected to an external resistor (1580Ω). The voltage drop across the resistor was recorded by a multimeter (Keithley 6517A, USA) controlled with LabView software at 15 min intervals.

Whenever the registered voltage of one MFC dropped down to 10 mV, the reactor was drained and fed it again with new water from the WWTP in order to keep the microorganism alive and carry on with the bioelectricity generation.

Once the voltage was stable and reproducible for several cycles, see Fig. 8, it was stabilized at its maximum value, and power density curves were measured by varying the external resistor over the range from 100 Ω to 20 kΩ. All experiments were carried out at room temperature, between 20 and 25 °C. It is important to mention that, the output values for both, power and voltage, are affected by the internal resistance of the device, which is detailed in Fig. 9.

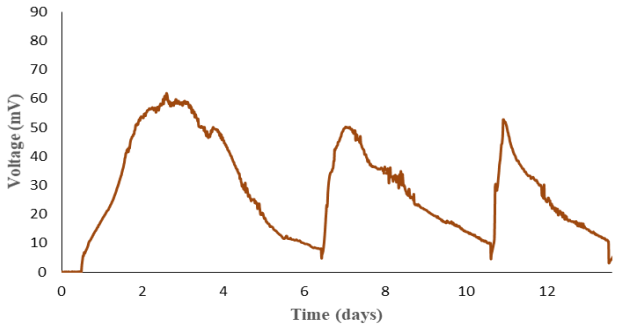

***Fig 8.**. Output voltage of the MFC D1 showing three cycles of feeding with wastewater from the primary clarifier effluent of a WWTP during a period of 13 days.*

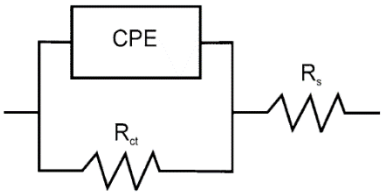

***Fig 9.**. Equivalent circuit of the MFC. Rct, Rs, and CPE correspond to charge transfer resistance, solution resistance, and constant phase element, respectively.*[7]

Previously in this report, the importance of the composition, morphology, and surface properties of anode materials have been commented. However, MFCs must be understood as a complete system where the electrochemical performance depends on both anode and cathode. On this basis, the experiment considers both electrodes and not only the anode where the bacteria attachment or the electron transfer occur.

Regarding the reduction process, as observed in Table V, MFCs with GNWs-based cathode presented a significant higher voltage than those with SS-mesh with MnO_2 electrodeposited which was below 100 mV. Among the samples with GNWs, those with MnO_2 electrodeposited on to the nanostructure surface delivered voltage values up to about 127 mV, and samples with GNWs-based cathodes from 115 up to about 150 mV.

Hence, the ORR taking place at the cathode is more efficient with GNWs than with electrodeposited MnO_2 decorating the substrate surface.

On the other hand, and concerning the oxidation process, the negative effect of the oxygen plasma treatment performed after the GNWs synthesis is demonstrated. It is generally accepted that this type of treatments results in an enhancement of the electrochemical properties since surface impurities are removed and step-like defects are generated inducing an improvement of the electron transfer kinetics [33]. However, the hydrophobicity of the sample is reduced, and this fact makes a higher impact on the final result insofar as the bacteria anchoring is reduced. Therefore, the complexity in order to generate the anode biofilm increases due to the surface oxygen functionalities, that reduce the electron transfer in the anode. This fact can be easily observed when the maximum voltage obtained for the type C MFC (116 mV) is compared to the type D MFCs value (152 mV). This MFCs have the same cathode configuration and the anode only differs on the plasma post-treatment, see table V.

Thus, the enhancement in the electrochemical properties of type D MFCs must be related with better bacteria attachment showed by the non-treated surface.

The power density of the samples follows the same trend, reaching up to 9 mW/m^2 in the case of the B-type MFCs (MnO_2-GNWs + O_2 plasma cathode and GNWs + O_2 plasma anode), as observed in Figure 10. Samples with GNWs-based cathode show an improvement in cell performance with respect to samples with MnO_2 electrodeposited on to the SS surface; 7 mW/m^2 for GNWs cathodes, and 3 mW/m^2 for MnO_2. Again, the sample without an O_2 plasma post-treatment performed in the anode presents a much higher value compared to its homologous, presumably due to the intact hydrophobic nature of the carbon-based substrate, which increases the affinity between the GNWs present in the anode and the microorganisms responsible for the bio-electricity generation, as mentioned above.

Finally, taking into account the electrons produced, we have estimated the amount of organic matter yielding electrons, effluent chemical oxygen demand (COD) and COD removal percentage, see Fig. 11.

In this case, the best results were obtained when using SS-mesh without GNWs as cathode and simply MnO_2 electrodeposited on the sample surface (89% COD removal) compared to samples with GNWs based-cathode (about 70%).

Nevertheless, while samples with MnO_2 on the cathode side lasted approximately for 15 days at a lower output voltage, samples with GNWs based-cathode lasted between 4-10 days at a higher voltage.

TABLE V
MAXIMUM MFCS VOLTAGE REGISTERED

MFCs	Cathode (SS-mesh)	Anode (SS-foil)	Maximum Voltage (mV)
A.1 A.2	MnO_2	GNWs + O_2 Plasma	84
B.1 B.2	MnO_2 / GNWs + O_2 Plasma	GNWs + O_2 Plasma	127
C.1 C.2	GNWs + O_2 Plasma	GNWs + O_2 Plasma	115
D.1 D.2	GNWs + O_2 Plasma	GNWs	152

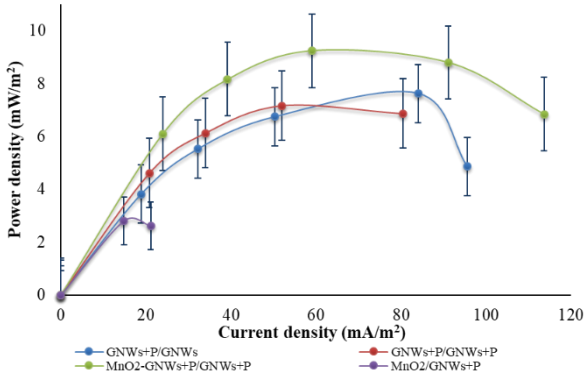

***Fig 10.**. Power density outputs of the different MFCs fed with the primary clarifier effluent of a municipal WWTP*

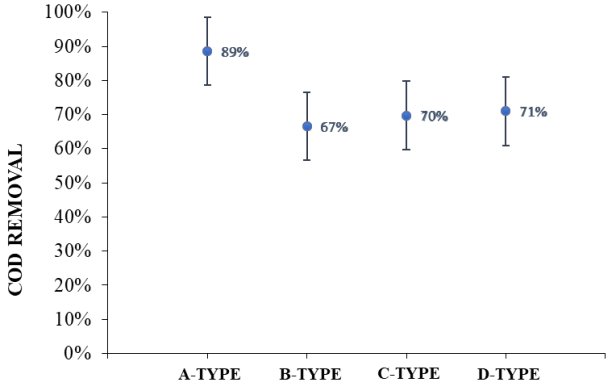

***Fig. 11.** Average values of the COD removal percentage for each type of MFC configuration.*

TABLE VI
COMPARISON BETWEEN THE OBTAINED RESULTS AND PREVIOUS STUDIES PERFORMED BY THE FEMAN RESEARCH GROUP [8].

MFCs	Cathode (SS-mesh)	Anode (SS-foil)	Maximum power density (mW/m^2)
Ref. [8].	VACNTs	VACNTs	14
B-type.	MnO_2 / GNWs + O_2 Plasma	GNWs + O_2 Plasma	9

Therefore, GNWs based-cathodes increase the electrochemical performance in comparison to MnO_2 electrodeposited on the substrate surface. However, the obtained results do not improve the previous studies performed by the *FEMAN* research [8], as observed in Table VI. The theoretical increase of the surface area provided by the GNWs on the anode side does not increase extracellular charge transport in comparison to vertically aligned carbon nanotubes (VACNTs). Using nanotubes on the anode a more efficient electric-generation from organic matter consumption occurred and a higher current was generated as it can be seen if the results are compared to the previous ones.

The reason behind this event could be related to the mechanisms by which bacteria transfer electrons to electrodes. The most widely accepted transfer mechanism proposed in previous reports is based on the use of extracellular polymeric substances (including filamentous) and bacterial nanowires [34].

Hence, the obtained results are in agreement with these proposed mechanisms, since the presence of GNWs at the anode does not increases direct contact with the electrode as much as VACNTs, and this requirement is extremely important to promote electron transfer [35].

VI. CONCLUSION

Graphene nanowalls were grown on 304 SS substrate and have been used as electrodes in air-cathode single chamber MFCs. Reductive pre-treatment and growth parameters have been optimized to obtain dense carbon nanostructures on both, SS foil and mesh, without losing the substrate properties. Furthermore, MnO_2 catalyst has been electrochemically deposited over SS-mesh and over SS-mesh decorated with GNWs to catalyze the ORR. It has been demonstrated the better performance of GNWs acting as cathode since the specific area of the electrode is increased. This electrochemical enhancement due to the enlarged surface area is not reproduced at the anode when the electrochemical performance of GNWs is compared with previous studies performed in the field based on VACNTs-electrodes. In this case, the improvement in the electrochemical measurements is not related with the presence of dense carbon nanostructures with high surface area but due to the electron transfer mechanism that take place in the biofilm located at the anode, enhanced by the direct contact with the electrode, as in the case of VACNTs. The O_2 plasma post-treatment performed usually after the carbon nanostructures growth in order to improve the hydrophilicity and thus the electrochemical properties, result in a worsened MFC system. Thereby, we can ensure that the microorganisms responsible for the bio-electricity generation prefer a hydrophobic substrate rather than hydrophilic. It is important to mention that this work has been done in half of the time of previous studies. Thus, it would be interesting to keep investigating and perform more experiments in order to confirm the extracted conclusions while trying to improve the electrochemical properties of the new systems. Growing carbon nanostructures relatively easily on a material as common as SS it is probably what makes this project appealing, since the potential for the future applications is outstanding. However, the technology is still not ready for making a step forward and scale up the production. More investment is needed, in terms of resources and time, in order to develop a MFC system based on carbon nanostructured electrodes with a real application in a WWTP like EDAR in Sant Feliu de Llobregat [19].

-ACKNOWLEDGMENT

The study has been supported by the project ENE2014-56109-C3-1-R and ENE2017-89210-C2-2-R of MICINN of Spanish Government, and 2014SGR0985 and 2017SGR1086 from the AGAUR of Generalitat de Catalunya. The authors thank Centres Científics i Tecnològics de la Universitat de Barcelona (CCiTUB) for measurement facilities and EDAR Sant Feliu de Llobregat for providing wastewater samples. M.F.M. acknowledges the financing from collaboration program grants of IN2UB.

REFERENCES

[1] S. J. Peighambardoust, S. Rowshanzamir, and M. Amjadi, "Review of the proton exchange membranes for fuel cell applications," *Int. J. Hydrogen Energy*, vol. 35, no. 17, pp. 9349–9384, 2010.

[2] L. Vasquez, "Fuel cell research," *Membr. Technol.*, vol. 1998, no. 95, p. 2, 2003.

[3] J. S. Lai and M. W. Ellis, "Fuel Cell Power Systems and Applications," *Proc. IEEE*, vol. 105, no. 11, pp. 2166–2189, 2017.

[4] N. Q. Minh, "System Designs and Applications," in *High-Temperature Solid Oxide Fuel Cells for the 21st Century: Fundamentals, Design and Applications: Second Edition*, 2015, pp. 283–328.

[5] K. Scott, "An Introduction to Microbial Fuel Cells," in *Microbial Electrochemical and Fuel Cells: Fundamentals and Applications*, Elsevier Ltd., 2015, pp. 3–27.

[6] P. Deepak, G. van Bogaert, L. Diels, and K. Vanbroekhoven, "A comparative assessment of bioelectrochemical systems and enzymatic fuel cells.," in *Microbial biotechnology: energy and environment*, 2012, pp. 39–57.

[7] R. Amade, M. Vila-Costa, S. Hussain, E. O. Casamayor, and E. Bertran, "Vertically aligned carbon nanotubes coated with manganese dioxide as cathode material for microbial fuel cells," *J. Mater. Sci.*, vol. 50, no. 3, pp. 1214–1220, 2015.

[8] R. Amade, H. A. Moreno, S. Hussain, M. Vila-Costa, and E. Bertran, "Vertically aligned carbon nanotubes as anode and air-cathode in single chamber microbial fuel cells," *Appl. Phys. Lett.*, vol. 109, no. 16, 2016.

[9] Y. Zhang *et al.*, "A graphene modified anode to improve the performance of microbial fuel cells," *J. Power Sources*, vol. 196, no. 13, pp. 5402–5407, 2011.

[10] Y. X. Huang *et al.*, "Graphene oxide nanoribbons greatly enhance extracellular electron transfer in bio-electrochemical systems," *Chem. Commun.*, vol. 47, no. 20, pp. 5795–5797, 2011.

[11] L. Xiao, J. Damien, J. Luo, H. D. Jang, J. Huang, and Z. He, "Crumpled graphene particles for microbial fuel cell electrodes," *J. Power Sources*, vol. 208, pp. 187–192, 2012.
[12] X. Zhang, S. Cheng, X. Wang, X. Huang, and B. E. Logan, "Separator characteristics for increasing performance of microbial fuel cells," *Environ. Sci. Technol.*, vol. 43, no. 21, pp. 8456–8461, Nov. 2009.
[13] M. Hiramatsu, H. Kondo, and M. Hori, "Graphene Nanowalls," in *New Progress on Graphene Research*, 2013, pp. 235–259.
[14] N. G. Shang *et al.*, "Catalyst-free efficient growth, orientation and biosensing properties of multilayer graphene nanoflake films with sharp edge planes," *Adv. Funct. Mater.*, vol. 18, no. 21, pp. 3506–3514, 2008.
[15] E. Luais *et al.*, "Carbon nanowalls as material for electrochemical transducers," *Appl. Phys. Lett.*, vol. 95, no. 1, 2009.
[16] Z. Wang, M. Shoji, and H. Ogata, "Carbon nanosheets by microwave plasma enhanced chemical vapor deposition in CH 4 -Ar system," *Appl. Surf. Sci.*, vol. 257, no. 21, pp. 9082–9085, 2011.
[17] M. M. Waje, X. Wang, W. Li, and Y. Yan, "Deposition of platinum nanoparticles on organic functionalized carbon nanotubes grown in situ on carbon paper for fuel cells," *Nanotechnology*, vol. 16, no. 7, pp. S395-400, Jul. 2005.
[18] T. Machino, W. Takeuchi, H. Kano, M. Hiramatsu, and M. Hori, "Synthesis of platinum nanoparticles on two-dimensional carbon nanostructures with an ultrahigh aspect ratio employing supercritical fluid chemical vapor deposition process," *Appl. Phys. Express*, vol. 2, no. 2, 2009.
[19] "EDAR Sant Feliu de Llobregat (Spain)," 2019. [Online]. Available: http://www.amb.cat/web/medi-ambient/aigua/instalacions-i-equipaments/detall/-/equipament/edar-de-sant-feliu-de-llobregat/274395/11818. [Accessed: 01-Jun-2019].
[20] R. Amade *et al.*, "Super-capacitive performance of manganese dioxide/graphene nano-walls electrodes deposited on stainless steel current collectors," *Materials (Basel).*, vol. 12, no. 3, pp. 1–13, 2019.
[21] A. M. Avetisyan, "Synthesis and characterization of multilayer graphene nanostructures," University of Barcelona, 2019.
[22] M. Hiramatsu, K. Shiji, H. Amano, and M. Hori, "Fabrication of vertically aligned carbon nanowalls using capacitively coupled plasma-enhanced chemical vapor deposition assisted by hydrogen radical injection," *Appl. Phys. Lett.*, vol. 84, no. 23, pp. 4708–4710, 2004.
[23] J. Ahmad, K. Bazaka, M. Oelgemöller, and M. Jacob, "Wetting, Solubility and Chemical Characteristics of Plasma-Polymerized 1-Isopropyl-4-Methyl-1,4-Cyclohexadiene Thin Films," *Coatings*, vol. 4, no. 3, pp. 527–552, 2014.
[24] S. Bhattacharya, A. Datta, J. M. Berg, and S. Gangopadhyay, "Studies on surface wettability of poly(dimethyl) siloxane (PDMS) and glass under oxygen-plasma treatment and correlation with bond strength," *J. Microelectromechanical Syst.*, vol. 14, no. 3, pp. 590–597, 2005.
[25] N. Tang, X. Tian, C. Yang, and Z. Pi, "Facile synthesis of α-MnO_2 nanostructures for supercapacitors," *Mater. Res. Bull.*, vol. 44, no. 11, pp. 2062–2067, 2009.
[26] E. Raymundo-Piñero, V. Khomenko, E. Frackowiak, and F. Béguin, "Performance of Manganese Oxide/CNTs Composites as Electrode Materials for Electrochemical Capacitors," *J. Electrochem. Soc.*, vol. 152, no. 1, p. A229, 2004.
[27] S.-C. Pang, M. A. Anderson, and T. W. Chapman, "Novel Electrode Materials for Thin-Film Ultracapacitors: Comparison of Electrochemical Properties of Sol-Gel-Derived and Electrodeposited Manganese Dioxide," *J. Electrochem. Soc.*, vol. 147, no. 2, p. 444, 2002.
[28] R. Amade, E. Jover, B. Caglar, T. Mutlu, and E. Bertran, "Optimization of MnO_2/vertically aligned carbon nanotube composite for supercapacitor application," *J. Power Sources*, vol. 196, no. 13, pp. 5779–5783, 2011.
[29] Z. Fan, J. Chen, B. Zhang, F. Sun, B. Liu, and Y. Kuang, "Electrochemically induced deposition method to prepare γ-MnO_2/multi-walled carbon nanotube composites as electrode material in supercapacitors," *Mater. Res. Bull.*, vol. 43, no. 8–9, pp. 2085–2091, 2008.
[30] S. Kurita *et al.*, "Raman spectra of carbon nanowalls grown by plasma-enhanced chemical vapor deposition," *J. Appl. Phys.*, vol. 97, no. 10, 2005.
[31] A. C. Ferrari *et al.*, "Raman spectrum of graphene and graphene layers.," *Phys. Rev. Lett.*, vol. 97, no. 18, p. 187401, 2006.
[32] M. Xu, L. Kong, W. Zhou, and H. Li, "Hydrothermal synthesis and pseudocapacitance properties of α-MnO_2 hollow spheres and hollow urchins," *J. Phys. Chem. C*, vol. 111, no. 51, pp. 19141–19147, 2007.
[33] S. C. Wang, K. S. Chang, and C. J. Yuan, "Enhancement of electrochemical properties of screen-printed carbon electrodes by oxygen plasma treatment," *Electrochim. Acta*, vol. 54, no. 21, pp. 4937–4943, 2009.
[34] N. S. Malvankar, M. T. Tuominen, and D. R. Lovley, "Comment on 'on electrical conductivity of microbial nanowires and biofilms' by S. M. Strycharz-Glaven, R. M. Snider, A. Guiseppi-Elie and L. M. Tender, Energy Environ. Sci., 2011, 4, 4366," *Energy Environ. Sci.*, vol. 5, no. 3, pp. 6247–6249, 2012.
[35] K. Rabaey *et al.*, "Microbial ecology meets electrochemistry: Electricity-driven and driving communities," *ISME J.*, vol. 1, no. 1, pp. 9–18, 2007.